

## 1 **Surface Sensing Stimulates Cellular Differentiation in *Caulobacter crescentus***

2 Rhett A. Snyder<sup>1,2†</sup>, Courtney K. Ellison<sup>1,3†</sup>, Geoffrey B. Severin<sup>4</sup>, Christopher M. Waters<sup>5</sup> and  
3 Yves V. Brun<sup>1,6\*</sup>

- 4
- 5 1. Department of Biology, Indiana University, 1001 E. 3<sup>rd</sup> Street, Bloomington, IN
  - 6 2. Current address: Johns Hopkins School of Medicine Medical Science Training Program,  
7 Johns Hopkins University, Baltimore, MD.
  - 8 3. Current address: Lewis-Sigler Institute for Integrative Genomics, Princeton University,  
9 Princeton, NJ.
  - 10 4. Department of Biochemistry and Molecular Biology, Michigan State University, East  
11 Lansing, MI, USA.
  - 12 5. Department of Microbiology and Molecular Genetics, Michigan State University, East  
13 Lansing, MI, USA.
  - 14 6. Département de microbiologie, infectiologie et immunologie, Université de Montréal,  
15 C.P. 6128, succ. Centre-ville, Montréal (Québec) H3C 3J7

16

17 †These authors contributed equally

18 \*Correspondence to: [yves.brun@umontreal.ca](mailto:yves.brun@umontreal.ca)

19

## 20 **Significance**

21 Cells from all domains of life sense and respond to mechanical cues [1–3]. In eukaryotes,  
22 mechanical signals such as adhesion and surface stiffness are important for regulating  
23 fundamental processes including cell differentiation during embryonic development [4]. While  
24 mechanobiology is abundantly studied in eukaryotes, the role of mechanical influences on  
25 prokaryotic biology remains under-investigated. Here, we demonstrate that mechanosensing  
26 mediated through obstruction of the dynamic extension and retraction of tight adherence (tad)  
27 pili stimulates cell differentiation and cell cycle progression in the dimorphic  $\alpha$ -proteobacterium  
28 *Caulobacter crescentus*. Our results demonstrate an important intersection between mechanical  
29 stimuli and the regulation of a fundamental aspect of cell biology.

30

31

## 32 **Abstract**

33 Cellular differentiation is a fundamental strategy used by cells to generate specialized  
34 functions at specific stages of development. The bacterium *C. crescentus* employs a specialized  
35 dimorphic life cycle consisting of two differentiated cell types. How environmental cues,  
36 including mechanical inputs such as contact with a surface, regulate this cell cycle remain  
37 unclear. Here, we find that surface sensing by the physical perturbation of retracting extracellular  
38 pilus filaments accelerates cell cycle progression and cellular differentiation. We show that  
39 physical obstruction of dynamic pilus activity by chemical perturbation or by a mutation in the  
40 outer membrane pilus pore protein, CpaC, stimulates early initiation of chromosome replication.  
41 In addition, we find that surface contact stimulates cell cycle progression by demonstrating that  
42 surface-stimulated cells initiate early chromosome replication to the same extent as planktonic  
43 cells with obstructed pilus activity. Finally, we show that obstruction of pilus retraction  
44 stimulates the synthesis of the cell cycle regulator, cyclic diguanylate monophosphate (c-di-  
45 GMP) through changes in the activity and localization of two key regulatory histidine kinases  
46 that control cell fate and differentiation. Together, these results demonstrate that surface contact  
47 and mechanosensing by alterations in pilus activity stimulate *C. crescentus* to bypass its  
48 developmentally programmed temporal delay in cell differentiation to more quickly adapt to a  
49 surface-associated lifestyle.

50

## 51 **Introduction**

52 In multicellular organisms, cellular differentiation is required for the formation of  
53 complex tissues and organs [5]. In unicellular organisms, the ability to coordinate and control  
54 specialized cell morphologies and functions is critical for niche survival in diverse environments

55 [6]. *C. crescentus* exhibits a dimorphic life cycle where asymmetric division results in the  
56 production of a non-reproductive, motile swarmer cell and a reproductive, non-motile stalked  
57 cell. In addition to their distinct reproductive states, each of these cell types possesses different  
58 polar structures. The swarmer cell is equipped with a single flagellum and multiple type IVc tight  
59 adherence (tad) pili at the same pole that are lost upon cellular differentiation into the stalked  
60 cell. Tad pili are subsequently replaced with a holdfast adhesin that mediates irreversible surface  
61 attachment and a thin cell-envelope extension called the stalk [7, 8].

62 Distinguishing characteristics between swarmer and stalked cells are partly due the action  
63 of the master response regulator, CtrA [8]. In swarmer cells, CtrA is phosphorylated and binds  
64 strongly to chromosomal sites near the origin of replication, preventing the initiation of DNA  
65 replication and thus locking cells in a non-reproductive, arrested G1 phase. During  
66 differentiation from swarmer to stalked cell, CtrA is dephosphorylated and proteolytically  
67 cleaved to allow for entry into S-phase and subsequent chromosome replication [8].

68 Regulatory control over differentiation is mediated by oscillating levels of c-di-GMP, a  
69 ubiquitous secondary messenger molecule that coordinates bacterial behavior in diverse species  
70 [9]. Newborn swarmer cells have low concentrations of c-di-GMP that slowly increase as they  
71 age. Between 20-40 mins post-division, a maximal level of c-di-GMP is observed, coinciding  
72 with holdfast synthesis and the transition from the motile to the sessile state. At the same time, a  
73 high level of c-di-GMP stimulates the dephosphorylation and deactivation of CtrA, allowing for  
74 chromosome replication as the swarmer cell differentiates [8].

75 c-di-GMP levels are controlled by the activity of the two histidine kinases PleC and DivJ,  
76 which localize at the swarmer and stalked pole of predivisional cells, respectively, and which  
77 dictate the distinct fates of the two progeny cells [10]. Delocalization of PleC and localization of

78 DivJ at the incipient stalked pole during cell differentiation mediate the activation of the  
79 diguanylate cyclase PleD by phosphorylation, resulting in an increase in c-di-GMP.

80         Although the signal transduction network governing the transition from swarmer to  
81 stalked cell has been well described, whether surface attachment impacts this process is not  
82 known. Here, we demonstrate that inhibition of dynamic pilus activity stimulates c-di-GMP to  
83 initiate stalked cell development. We show that physical obstruction of pilus retraction and  
84 surface contact stimulate the initiation of DNA replication. We show that a mutation in the outer  
85 membrane pilus pore protein CpaC that partially disrupts pilus retraction stimulates holdfast  
86 synthesis and initiation of DNA replication in a Pila-dependent fashion. Finally, we show that  
87 physical obstruction of pilus retraction directly stimulates c-di-GMP synthesis by accelerating  
88 the delocalization of PleC and localization of DivJ at the incipient stalked pole, key steps in the  
89 activation of PleD and the production of c-di-GMP. Thus, by stimulating the synthesis of the  
90 holdfast [11] and cell differentiation, surface contact ensures that the permanently attached cell  
91 enters the stalked phase, which is best adapted for nutrient uptake on a surface [12].

92

## 93 **Results**

### 94 **Obstruction of pilus retraction stimulates DNA replication initiation.**

95         Whether mechanical inputs can stimulate *C. crescentus* cell differentiation is unknown.  
96 Previous work has demonstrated that *C. crescentus* swarmer cells produce holdfast in response to  
97 surface contact independent of cell age [11, 13, 14], and recent findings suggests that this  
98 surface-stimulated holdfast synthesis is mediated by changes in type IVc tad pili dynamic  
99 activity upon binding of pili to a surface [11]. *C. crescentus* tad pili exhibit dynamic cycles of  
100 extension and retraction by polymerization and depolymerization of the major pilin subunit,

101 PilA. Visualization of pili and their dynamic activity is achieved through knock-in cysteine  
102 mutation in PilA (Pil-cys) followed by the addition of thiol-reactive maleimide conjugates [11,  
103 15, 16]. Dynamic activity of pilus fibers can be obstructed by the addition of bulky maleimide  
104 conjugates like polyethylene glycol maleimide (PEG-mal) to Pil-cys strains. In *C. crescentus*,  
105 obstruction of dynamic pilus activity through this method stimulates holdfast synthesis in the  
106 absence of surface contact, suggesting that the tension on surface-bound, retracting tad pili  
107 stimulates bacterial mechanosensing [11].

108         Because cell-cycle progression and cellular differentiation is concomitant with holdfast  
109 synthesis in planktonic cells, we hypothesized that surface contact may also accelerate the *C.*  
110 *crescentus* life cycle. A key marker for cell cycle progression is the initiation of DNA  
111 replication. We reasoned that should surface sensing stimulate initiation of DNA replication,  
112 cells with obstructed pili dynamics would have a higher DNA content compared to non-  
113 stimulated cells. To test this hypothesis, we incubated wild-type (WT) or Pil-cys cells with or  
114 without PEG-mal followed by rifampicin treatment to prevent new initiation of DNA replication  
115 while allowing for the completion of rounds of DNA replication that had already been initiated.  
116 We then labeled genomic DNA of treated cell cultures using SYTOX DNA-intercalating  
117 fluorescent dye and performed flow cytometry to quantify the DNA content of populations of  
118 cells. Swarmer cells arrested in the G1 phase harbor a single chromosome (1N), whereas cells  
119 that initiate chromosome replication prior to rifampicin treatment possess two chromosomes  
120 (2N). WT populations and untreated populations of the Pil-cys strain exhibited a ~2-fold ratio of  
121 2N:1N chromosome content. In contrast, the Pil-cys population treated with PEG-mal exhibited a  
122 ~3-fold ratio of 2N:1N chromosome content (Figure 1A and B). Importantly, Pil-cys cells treated  
123 with polyethylene glycol lacking the thiol-reactive maleimide group (PEG) exhibited a ratio of

124 2N:1N genomic content similar to WT cells and untreated pil-cys cells. These results suggest  
125 that obstruction of pili dynamics stimulates the initiation of DNA replication.

126 To confirm the above results, we tracked chromosome replication at the single-cell level.  
127 During S phase, the chromosomal partitioning system *parABS* in *C. crescentus* is involved in  
128 chromosome segregation. ParB dimers bind *parS* sequences adjacent to the origin of replication  
129 and subsequent interactions with cytoplasmic ParA helps to physically migrate the ParB-*parS*-  
130 DNA complex across the length of the cell [17]. To determine whether obstruction of pilus  
131 dynamics stimulates the initiation of DNA replication, we tracked the localization of the ParB in  
132 cells obstructed for pilus retraction with PEG-mal. For cells in G1 phase, a single ParB focus is  
133 observed at the flagellar pole where the origin of replication is localized. After initiation of DNA  
134 replication, a second ParB focus appears as newly-synthesized *parS* sites are bound by ParB  
135 dimers and translocated to the opposite cell pole. We thus examined the percentage of piliated  
136 cell with two ParB foci as a marker for cells that had initiated DNA replication. When treated  
137 with PEG-mal, the Pil-cys strain exhibited a 20% increase in the number of piliated cells with  
138 two ParB foci as compared to untreated and PEG-treated cells (Figure 1C). Taken together, these  
139 results suggest that obstruction of pili dynamics stimulates entry into the cell cycle.

140

141 **A mutation in the outer membrane pilus secretin that disrupts pilus retraction stimulates**  
142 **holdfast synthesis and initiation of DNA replication.**

143 Because chemical obstruction of pilus retraction through the addition of PEG-mal  
144 stimulates initiation of DNA replication, we reasoned that some mutants genetically deficient in  
145 pilus retraction would exhibit a similar phenotype. Since pili are terminally retracted prior to  
146 cellular differentiation, we hypothesized that stalked cells of a retraction mutant would exhibit an

147 increase in the number of cells with pili localized at the tips of stalks where the outer membrane  
148 secretin CpaC remains after stalk synthesis [18]. Because retraction mutants in several species  
149 are hyperpiliated and hyperpiliation results in increased surface attachment, we performed an  
150 unbiased genetic screen to enrich for mutants that attach more efficiently to surfaces. We then  
151 screened the enriched cell population for changes in pilus-dependent  $\phi$ CbK phage sensitivity  
152 because we assumed that a mutant deficient in pilus dynamics would be more resistant to pilus-  
153 dependent phage infection. From this screen, we isolated a mutant that harbored pili at the tips of  
154 stalked cells, indicative of obstructed pilus retraction and a failure to terminally retract its pili  
155 prior to cellular differentiation (Figure 2A and B). Whole genome sequencing revealed a  
156 mutation that mapped to the outer membrane pilus secretin gene, *cpaC*<sup>G324D</sup>.

157 To test whether the obstruction of pilus retraction mediated by the *cpaC*<sup>G324D</sup> mutation  
158 stimulates cell cycle progression similarly to physical obstruction by PEG-mal treatment, we first  
159 quantified holdfast synthesis in mutant populations. In the *cpaC*<sup>G324D</sup> mutant, approximately 36%  
160 of synchronized cells produced a holdfast within five minutes of birth as compared to 17% in  
161 cells with the wild-type allele of *cpaC* (Figure 2C). By comparison, 51% of cells obstructed for  
162 pilus retraction by the addition of PEG-mal synthesize a holdfast within five minutes of birth.  
163 These results suggest that the *cpaC*<sup>G324D</sup> mutant is partially stimulated for surface sensing.  
164 Interestingly, the *cpaC*<sup>G324D</sup> mutant appears only partially obstructed for pilus retraction as  
165 evidenced by fluorescent cell bodies (Figure 2A). Indeed, we have previously shown that cell  
166 body fluorescence in pil-cys cells labeled with fluorescent maleimide is dependent upon pilus  
167 retraction and dispersal of labeled pilins into an inner membrane pilin pool [11]. As the  
168 *cpaC*<sup>G324D</sup> mutant exhibits both cell body fluorescence as well as pili at the tips of stalks, we infer  
169 that it is only partially obstructed for pilus retraction.

170 To test whether the *cpaC*<sup>G324D</sup> mutant had an increase in DNA replication initiation  
171 similar to cells physically obstructed for pilus retraction, we measured the DNA content of  
172 *cpaC*<sup>G324D</sup> mutants. We found that the *cpaC*<sup>G324D</sup> mutant had an intermediate increase in the  
173 number of cells harboring two chromosomes compared to the PEG-mal treated pil-cys strain and  
174 WT, indicative of accelerated cell-cycle progression (Figure 2D). Importantly, a *cpaC*<sup>G324D</sup> *pilA*  
175 double mutant lacking the major pilin subunit exhibited the same phenotype as a *pilA* mutant  
176 alone, demonstrating a dependence of cell-cycle acceleration of the *cpaC*<sup>G324D</sup> mutant on the  
177 presence of PilA. These results suggest that obstruction of pili dynamics by the *cpaC*<sup>G324D</sup>  
178 mutation stimulates both holdfast synthesis and entry into the cell cycle.

179

#### 180 **Surface contact stimulates cell cycle progression.**

181 While physical obstruction of pilus retraction with PEG-mal or by *cpaC* mutation is  
182 inferred to simulate surface sensing in the absence of a surface, we sought to directly test  
183 whether surface contact stimulates cell cycle entry. Because cultures of *C. crescentus* harbor a  
184 mixture of undifferentiated swarmer cells, stalked cells, and predivisional cells at various stages  
185 of replication, we synchronized cultures of cells using a plate synchrony method to isolate  
186 newborn swarmer cells. We then tracked the timing of ParB duplication in surface-attached,  
187 planktonic, and PEG-mal treated planktonic populations (Figure 3A). Attached cells and  
188 planktonic cells treated with PEG-mal displayed similar ParB duplication times of 17 and 16.4  
189 min after birth respectively, while untreated planktonic cells displayed a delay in ParB  
190 duplication of 19.7 min after birth (Figure 3B and C). Notably, the *cpaC*<sup>G324D</sup> mutant that is  
191 genetically obstructed for pilus retraction exhibited ParB duplication at 17.6 minutes after birth,  
192 similar to both attached and PEG-mal-treated cells.



193 Taken together, our results indicate that swarmer cells that contact a surface, planktonic  
194 swarmer cells physically obstructed for pilus retraction, and planktonic swarmer cells with a  
195 mutation that obstructs pilus retraction differentiate ~15% earlier than planktonic swarmer cells.  
196 We next sought to determine the mechanism by which obstruction of pili dynamics stimulates  
197 entry into the cell cycle.

198

199 **Obstruction of pilus retraction stimulates c-di-GMP synthesis by altering the**  
200 **activity of developmental regulators.**

201 The initiation of DNA replication and polar differentiation are tightly coupled during  
202 swarmer cell differentiation. This coupling is mediated in part by the histidine kinases PleC and  
203 DivJ, which antagonistically regulate the phosphorylation state of the single domain response  
204 regulator DivK in order to control entry into the cell cycle and the phosphorylation of PleD to  
205 stimulate c-di-GMP synthesis [19]. It was previously demonstrated that PleD is important for  
206 surface contact stimulation of holdfast synthesis [11], suggesting an increase of c-di-GMP upon  
207 surface sensing. We thus measured c-di-GMP concentrations of cell populations after obstruction  
208 of pilus activity (Figure 4A). WT cells lacking the Pil-cys mutation were unaffected by PEG-mal  
209 treatment while the Pil-cys strain exhibited a 50% increase in c-di-GMP concentration upon  
210 obstruction of pilus retraction. These results suggest that surface sensing by obstruction of pilus  
211 retraction is sufficient to stimulate the production of c-di-GMP.

212 c-di-GMP synthesis by PleD is spatially and temporally controlled by PleC and DivJ.  
213 Conveniently, the subcellular localization of PleC and DivJ correlates with their activity [8][19].  
214 PleC is localized at the flagellar pole in swarmer cells where it acts as a phosphatase for DivK  
215 and PleD. PleC delocalizes and switches to a kinase during differentiation from the swarmer to

216 stalked cell. During differentiation, DivJ interacts with its localization and activation factor  
217 SpmX to localize to the incipient stalked pole, where it phosphorylates DivK and PleD to start  
218 the cell cycle and stimulate cell differentiation [8]. To determine if surface sensing regulates this  
219 key regulatory switch, we tracked changes in PleC and DivJ localization in cells with obstructed  
220 pilus retraction as a proxy for their activity (Figure 4). Strains containing PleC-YFP or DivJ-CFP  
221 were treated with maleimide dye with or without PEG-mal, and piliated cells were tracked for  
222 changes in protein localization over time. The PEG-treated control and untreated Pil-cys  
223 populations exhibited a 20% increase in the number of cells with delocalized PleC by 60 min,  
224 while ~60% of cells treated with PEG-mal delocalized PleC by the same time, demonstrating an  
225 acceleration in the PleC switch from phosphatase to kinase activity upon disruption of pilus  
226 dynamics (Figure 4B and D). DivJ also localized to the incipient stalked pole up to 20 min earlier  
227 in PEG-mal-treated samples in comparison to untreated or PEG-treated cells, showing that DivJ  
228 kinase activation is triggered by obstruction of pilus retraction (Figure 4C and E). These results  
229 demonstrate that the PleC-DivJ cell differentiation switch is stimulated by the obstruction of  
230 pilus retraction in addition to DNA replication and holdfast synthesis. Thus, mechanical cues  
231 upon surface contact stimulate differentiation of swarmer cells into stalked cells, which are better  
232 adapted for nutrient uptake on a surface [12].

233

## 234 **Discussion**

235 It is becoming clear that mechanical signals from the environment have substantial  
236 impact on cell biology [20–22]. The mechanobiology of bacteria is an emerging field where we  
237 know little about the processes that can be modulated by mechanical signals and about how the  
238 signals are sensed and transduced. Here, we demonstrate that the mechanical cue of surface

239 contact stimulates bacterial cell cycle progression and cell differentiation. We show that  
240 perturbation of pilus dynamic activity through surface contact, physical obstruction, or mutation  
241 of the pilus outer membrane pore stimulates DNA replication initiation and that physical  
242 obstruction of pilus dynamics causes a spike in c-di-GMP synthesis. These results suggest that  
243 surface contact causes an increase of c-di-GMP as a consequence of perturbation of pili  
244 dynamics and that this increase in c-di-GMP stimulates cell cycle progression and cell  
245 differentiation. It was previously shown that PleD is the main diguanylate cyclase responsible for  
246 the increase of c-di-GMP during swarmer to stalked cell differentiation [19]. C-di-GMP  
247 production by PleD stimulates the ShkA-TacA phosphorylation cascade, ultimately creating a  
248 positive feedback loop that results in increased PleD activity and ensures irreversible  
249 commitment to cell differentiation [23]. The activity of PleD is modulated by the histidine  
250 kinases PleC and DivJ, whereby PleC dephosphorylates PleD to inhibit its activity and DivJ  
251 phosphorylates PleD to activate it [19]. Delocalization of PleC and localization of DivJ at the  
252 incipient stalked pole result in an increase in PleD phosphorylation and c-di-GMP level, which  
253 triggers cell differentiation. PleC and DivJ similarly antagonistically modulate the  
254 phosphorylation state of the single domain response regulator DivK to ultimately control CtrA  
255 activity and chromosome replication [19]. We show that obstruction of pilus dynamics  
256 accelerates delocalization of PleC and localization of DivJ at the incipient stalked pole, which is  
257 expected to increase c-di-GMP and thereby stimulate entry into the cell cycle and cell  
258 differentiation (Figure 5). At the same time, surface contact also stimulates holdfast synthesis  
259 through flagellum motor interference and obstruction of pili dynamics, causing a spike in c-di-  
260 GMP that allosterically activates the holdfast polysaccharide glycosyltransferase HfsJ to  
261 stimulate holdfast synthesis [11, 13, 14].

262           When newborn swarmer cells swim to a surface, the DivJ kinase is not yet localized nor  
263 active [24] and PleC is localized at the pole bearing pili and the flagellum where it acts as a  
264 phosphatase to dephosphorylate PleD, preventing its activation and localization [19]. The  
265 accelerated delocalization of PleC and its concomitant switch to a kinase is therefore likely to be  
266 the first step in the stimulation of PleD activity. Furthermore, the elevation of DivK~P  
267 concentration stimulates DivJ kinase, causing a positive feedback loop between PleC and DivJ  
268 that leads to an increase in both DivK~P and PleD~P [19]. This synergy is also likely potentiated  
269 by PleC's positive action on the localization and activation of DivJ by SpmX [24]. The co-  
270 localization of PleC with the pili and flagellum suggests that there may be crosstalk between the  
271 two surface contact sensory systems and PleC, providing an integration of holdfast synthesis,  
272 initiation of DNA replication, and cell differentiation upon surface contact. In support of this  
273 model, data from a parallel study by Del Medico et al. suggest that a PilA signal sequence is  
274 involved in stimulating c-di-GMP synthesis to trigger cell cycle progression through the PleC-  
275 PleD signaling cascade [25]. From an ecological perspective, accelerated cellular differentiation  
276 after surface contact and permanent attachment likely benefits *C. crescentus* by activating the  
277 pathway that stimulates stalk synthesis. Indeed, the synthesis of a thin stalk is thought to improve  
278 nutrient uptake capacity in the diffusion-limited environment of a surface [12, 26]. A recent  
279 study demonstrated that some bacteria can sense and respond to changes in liquid flow rates [21],  
280 and accelerated stalk synthesis may also provide an advantage to surface-associated cells by  
281 allowing better access to environmental flow conditions [27].

282           Finally, our results are an important milestone in understanding how cells sense and  
283 respond to their environments by highlighting that physical cues can influence the hardwired  
284 circuitry of cellular differentiation and reproduction. Elucidating how cells sense and transduce

285 the inputs from mechanical stimuli will be critical for determining how mechanical stimuli  
286 influence intracellular processes.

287

## 288 **Materials and methods**

### 289 **Bacterial strains, plasmids, and growth conditions.**

290 Bacterial strains and primers used in this study are listed in Supplemental Table 1. *C.*  
291 *crenscentus* strains were grown at 30°C in peptone yeast extract (PYE) medium [28]. *Escherichia*  
292 *coli* DH5 $\alpha$  (Bioline) were used for cloning and grown in lysogeny broth (LB) medium at 37°C  
293 supplemented with 25  $\mu$ g/ml kanamycin when appropriate.

294 Plasmids were transferred to *C. crescentus* by electroporation, transduction with  $\Phi$ Cr30  
295 phage lysates, or conjugation with S-17 *E. coli* strains as described previously [29]. In-frame  
296 allelic substitutions were made by double homologous recombination using pNPTS-derived  
297 plasmids as previously described [30]. Briefly, plasmids were introduced to *C. crescentus* and  
298 then two-step recombination was performed using sucrose and kanamycin resistance or  
299 sensitivity as a selection for each step. Mutants were verified through a combination of  
300 sequencing and microscopy phenotyping.

301 For construction of the pNPTS-derived plasmids, ~500 bp flanking regions of DNA on  
302 either side of the desired mutations were amplified from *C. crescentus* genomic DNA. Point  
303 mutations were built into the UpR and DownF primers as indicated in Supplemental Table 1.  
304 Upstream regions were amplified using UpF and UpR primers while downstream regions were  
305 amplified using DownF and DownR primers. The resulting DNA was purified (Qiaquick, Zymo  
306 Research) and assembled in pNPTS138 that had been digested with restriction enzyme *EcoRV*  
307 (New England Biolabs) using HiFi Assembly Master Mix (New England Biolabs). For

308 construction of pNPTS138*hfsA*<sup>+</sup>, the entire *hfsA* gene and ~500 bp of both up and downstream  
309 flanking DNA was amplified from strain FC764 [31] and cloned into pNPTS138 as described  
310 above for use in restoring holdfast synthesis in NA1000 strains.

### 311 **Cyclic-di-GMP quantification.**

312 Cyclic di-GMP was quantified as described previously [32]. Briefly, strains were grown  
313 to early-log growth phase (OD<sub>600</sub> 0.15-0.25) in PYE medium. One ml of culture was centrifuged  
314 for five min at 21,000 x g and the supernatant was removed. Cell pellets were resuspended in  
315 200 µl cold extraction buffer (1:1:1 mix of methanol, acetonitrile, and distilled H<sub>2</sub>O + 0.1 M  
316 formic acid) and incubated at -20°C for 30 min. Samples were then centrifuged at 21,000 x g to  
317 pellet cell debris, and the supernatant was transferred to a fresh tube and stored at -80°C until  
318 use. Experimental extraction solutions were desiccated overnight in a SpeedVac, re-solubilized  
319 in 100 µl of ultrapure water, briefly vortexed and centrifuged for 5 min at 21,000 x g to pellet  
320 insoluble debris. The clarified extract solutions were transferred to sample vials and analyzed by  
321 UPLC-MS/MS in negative ion-mode electrospray ionization with multiple-reaction monitoring  
322 using an Acquity Ultra Performance LC system (Water Corp.) coupled with a Quattro Premier  
323 XE mass spectrometer (Water Corp.) over an Acquity UPLC BEH C18 Column, 130 angstrom,  
324 1.7 µm, 2.1 mm x 50 mm. c-di-GMP was identified using precursor > product masses of 689.16  
325 > 344.31 with a cone voltage of 50.0 V and collision energy of 34.0 V. Quantification of c-di-  
326 GMP in sample extracts was determined using a standard curve generated from chemically  
327 synthesized c-di-GMP (AXXORA). The standard curve solutions were prepared using twofold  
328 serial dilutions of c-di-GMP (1.25 µM – 19 nM) in ultra-pure water that were further diluted 1:10  
329 into biological extracts (final c-di-GMP concentrations: 125 nM to 1.9 nM) from a low c-di-  
330 GMP strain of *C. crescentus* lacking several diguanylate cyclases (c-di-GMP<sup>0</sup>) described

331 previously [9] which had been grown, harvested, extracted, desiccated and solubilized in ultra-  
332 pure water in tandem with the experiments samples described above. General UPLC buffer  
333 preparations, chromatographic gradients and MS/MS parameters were performed using a  
334 previously published method [33]. Intracellular concentrations of c-di-GMP were calculated as  
335 described previously [34] assuming *C. crescentus* average cellular volume of  $6.46 \times 10^{-16}$  L. The  
336 total number of cells present in each extraction was calculated by normalizing OD<sub>600</sub> for each  
337 sample to the average CFUs found for NA1000 cultures grown to an OD<sub>600</sub> 0.2 ( $2 \times 10^9$   
338 CFU/ml).

### 339 **Quantification of piliated cells with two ParB foci.**

340 Bacterial cultures were grown to an OD<sub>600</sub> of 0.2-0.4 and labeled for pili as described  
341 previously [11]. Briefly, 100 µl of cultures were labeled with 25 µg/ml AlexaFluor 488 C<sub>5</sub>  
342 maleimide dye (AF488-mal)(ThermoFisher) for five min at room temperature. To block pilus  
343 retraction, cells were incubated simultaneously with AF488-mal and 500 µM of  
344 methoxypolyethylene glycol maleimide (5000 Da)(PEG-mal)(Sigma) for five min at room  
345 temperature. Cells were centrifuged at 5,200 x g for one min, the supernatant was discarded, and  
346 the pellet was then washed with 100 µl of PYE and centrifuged again. The supernatant was  
347 removed, and the cells were concentrated in 5-8 µl of PYE. One µl of washed, labeled cells was  
348 spotted onto a 60 x 22 glass coverslip and imaged under a 1% agarose (SeaKem) pad made with  
349 sterile, distilled water before imaging. Imaging was performed on an inverted Nikon Ti-2  
350 microscope using a Plan Apo 60X objective, a GFP/DsRed filter cube, a Hamamatsu  
351 ORCAFlash4.0 camera, and Nikon NIS Elements Imaging Software. Quantification of piliated  
352 cells and number of ParB foci was performed manually using NIS Elements Analysis software.

### 353 **Quantification of genomic content in populations of cells.**

354 Bacterial cultures were grown to an OD<sub>600</sub> of 0.2-0.4 and were left untreated or were  
355 treated with either 500 μM of PEG5000-mal or 500 μM polyethylene glycol (~5000 Da)(Sigma).  
356 After pilus treatment, cells were incubated with 15 μg/ml of rifampicin for 3 h to prevent new  
357 cycles of DNA initiation. 1.5 ml of culture was concentrated into 180 μl PBS (phosphate  
358 buffered saline) and fixed with 420 μl 100% ethanol at 4°C for one hour. After fixation, cells  
359 were centrifuged at 5,200 x g and washed once with 600 μl PBS. Cells were finally resuspended  
360 in 600 μl PBS and 2.5 μM SYTOX Green Nucleic Acid Stain (Thermofisher) was added  
361 preceding stationary incubation overnight at 4°C. Fluorescence intensity and light scattering  
362 were quantified by flow cytometry using the FACSCalibur at the IUB FACS facility and data  
363 were analyzed using FlowJo software.

#### 364 **Quantification of PleC and DivJ localization patterns.**

365 Pili were labeled with AF594-mal (Thermofisher) and treated with either PEG-mal or  
366 PEG as described above. For tracking DivJ-CFP localization after pilus treatment, cells were  
367 placed in a static, 30°C incubator. Every 10 min, one μl of sample was spotted onto a glass  
368 coverslip and imaged using DsRed/CFP filter settings under 1% agarose pads made with sterile,  
369 distilled water as described above. For tracking PleC delocalization, cells were spotted onto a  
370 glass coverslip and placed under a 1% agarose pad made with PYE and an initial image was  
371 taken using DsRed filter settings to identify piliated cells. Cells were then imaged using YFP  
372 filter settings every two min to track PleC-YFP delocalization. Quantification of piliated cells  
373 with delocalized PleC or localized DivJ was performed manually using NIS Elements Analysis  
374 software.

#### 375 **Identification of mutant deficient in pilus retraction.**



376 A subculture-based forward genetic screen was performed to enrich for mutants efficient  
377 in holdfast-independent surface attachment. Ten replicates of a parent Pil-cys strain lacking the  
378 holdfast-synthesizing genes ( $\Delta hfsDAB$ ) was grown in five ml of PYE in glass tubes to stationary  
379 phase. Cultures were then dumped and lightly washed with PYE to remove loosely bound cells.  
380 The tubes were then refilled with five ml of PYE and again grown to stationary phase, and this  
381 was repeated until turbid growth was observed after overnight growth (23 days). Cultures were  
382 then streaked out onto PYE agar plates to isolate individual mutants. Isolates were then tested for  
383 changes in phage sensitivity to the pilus-dependent phage  $\Phi$ CbK, and those exhibiting an  
384 alteration from wildtype sensitivity were sequenced to identify mutations. Whole genome  
385 sequencing and mutant identification was performed as described previously [35] with the  
386 exception that sequencing reads were mapped to the genome of *C. crescentus* NA1000  
387 (NC\_011916.1).

#### 388 **Phage sensitivity assays.**

389 Phage sensitivity assays were performed as described previously [36]. Briefly, five  $\mu$ l of  
390  $\Phi$ CbK phage dilutions were spotted onto lawns of growing *C. crescentus* strains. Lawns were  
391 made by adding 200  $\mu$ l of stationary phase cultures to three ml of melted top agar (0.5% agar in  
392 PYE) and spread over 1.5% PYE agar plates. After the top agar solidified, five  $\mu$ l of phage  
393 dilutions in PYE were spotted on top. Plates were grown for two days at 30°C before imaging.

#### 394 **Cell synchronization and surface stimulation experiments.**

395 Cells were synchronized as described previously [11] with some modifications. Briefly,  
396 50 ml of PYE in a 15 cm polystyrene petri dish was inoculated with one ml of overnight culture  
397 of the indicated holdfast-synthesizing strain expressing ParB-mCherry and incubated for 16 h at  
398 room temperature at 70 rpm on an orbital shaker. Four hours prior to experiments, the petri dish

399 was washed with 50 ml of sterile, distilled water. 50 ml of PYE medium was added to the petri  
400 dish and incubated at room temperature shaking for an additional four hours. Just before use, the  
401 petri plate was washed twice with 100 ml of distilled water, and then one ml of PYE (containing  
402 500  $\mu$ M PEG-mal where indicated) was added to the petri plate and harvested after one minute to  
403 collect newborn swarmer cells. For planktonic populations, the one ml of PYE containing  
404 newborn swarmer cells was added to a 1.7 ml centrifuge tube and left stationary at room  
405 temperature for three minutes before 1  $\mu$ l was spotted onto a coverslip and imaged under a 1%  
406 agarose pad made with PYE and containing 0.5  $\mu$ g/ml AF488-WGA to label holdfasts. For  
407 surface-attached cells, 1  $\mu$ l of the harvested newborn swarmer cells was spotted onto a glass  
408 coverslip and left stationary at room temperature for three minutes before the addition of the 1%  
409 agarose pad. Agarose pads do not stimulate surface-contact responses as reported elsewhere [32],  
410 and we found that allowing cells to attach to the glass coverslip for three minutes before the  
411 addition of the pad was critical for observing a surface-stimulated response. Time-lapse images  
412 of ParB-mCherry foci and holdfasts labeled with AF488-WGA in the agarose pad were captured  
413 once per minute over 35 min using the same settings described above. Holdfast and ParB-  
414 mCherry duplication events were quantified manually using NIS Elements Analysis software.

415

## 416 **Acknowledgements**

417 We thank A. Dalia and C. Berne and members of the Gitai lab for helpful discussions  
418 regarding the manuscript. We thank the Center for Genomics and Bioinformatics at Indiana  
419 University for whole genome sequencing and SNP mutant identification. We also thank the  
420 FACS Core Facility at IUB for training and assistance in flow cytometry experiments. We thank  
421 D. Kysela for construction of strain YB7341. **Funding:** This study was supported by grant

422 R35GM122556 from the National Institutes of Health and by a Canada 150 Research Chair in  
423 Bacterial Cell Biology to YVB, by grant R01GM109259 from the National Institutes of Health  
424 to CMW, and by National Science Foundation fellowship 1342962 to CKE; **Author**  
425 **contributions:** RAS, CKE, GBS, CMW and YVB designed the experiments. RAS, CKE, and  
426 GBS performed the experiments. All authors analyzed the data. RAS, CKE, and YVB wrote the  
427 manuscript. All authors contributed to editing the manuscript; **Competing interests:** The authors  
428 declare no competing interests; and **Data and materials availability:** All data is available in the  
429 main text or the supplementary materials.

430

431

432

### 433 **References**

- 434 1. Eyckmans J, Boudou T, Yu X, Chen CS (2011) A Hitchhiker's Guide to Mechanobiology.  
435 *Dev Cell* 21:35–47. <https://doi.org/10.1016/j.devcel.2011.06.015>
- 436 2. Discher DE, Janmey P, Wang Y-L (2005) Tissue Cells Feel and Respond to the Stiffness  
437 of Their Substrate. *Science* (80- ) 310:1139–1143.  
438 <https://doi.org/10.1126/science.1116995>
- 439 3. Hoffman BD, Grashoff C, Schwartz MA (2011) Dynamic molecular processes mediate  
440 cellular mechanotransduction. *Nature* 475:316–323. <https://doi.org/10.1038/nature10316>
- 441 4. Engler AJ, Sen S, Sweeney HL, Discher DE (2006) Matrix Elasticity Directs Stem Cell  
442 Lineage Specification. *Cell* 126:677–689. <https://doi.org/10.1016/J.CELL.2006.06.044>
- 443 5. Sánchez Alvarado A, Yamanaka S (2014) Rethinking Differentiation: Stem Cells,  
444 Regeneration, and Plasticity. *Cell* 157:110–119.  
445 <https://doi.org/10.1016/J.CELL.2014.02.041>
- 446 6. Shapiro L, Agabian-Keshishian N, Bendis I (1971) Bacterial differentiation. *Science*  
447 173:884–92. <https://doi.org/10.1126/SCIENCE.173.4000.884>
- 448 7. Toh E, Kurtz Jr. HD, Brun YV (2008) Characterization of the *Caulobacter crescentus*  
449 holdfast polysaccharide biosynthesis pathway reveals significant redundancy in the  
450 initiating glycosyltransferase and polymerase steps. *J Bacteriol* 190:7219–7231.

- 451 <https://doi.org/JB.01003-08> [pii]10.1128/JB.01003-08
- 452 8. Curtis PD, Brun YV (2010) Getting in the loop: regulation of development in *Caulobacter*  
453 *crescentus*. *Microbiol Mol Biol Rev* 74:13–41. <https://doi.org/10.1128/MMBR.00040-09>
- 454 9. Abel S, Bucher T, Nicollier M, et al (2013) Bi-modal distribution of the second messenger  
455 c-di-GMP controls cell fate and asymmetry during the *caulobacter* cell cycle. *PLoS Genet*  
456 9:e1003744. <https://doi.org/10.1371/journal.pgen.1003744>
- 457 10. Kirkpatrick CL, Viollier PH (2012) Decoding *Caulobacter* development. *FEMS*  
458 *Microbiol Rev* 36:193–205. <https://doi.org/10.1111/j.1574-6976.2011.00309.x>
- 459 11. Ellison CK, Kan J, Dillard RS, et al (2017) Obstruction of pilus retraction stimulates  
460 bacterial surface sensing. *Science* 358:535–538. <https://doi.org/10.1126/science.aan5706>
- 461 12. Wagner JK, Setayeshgar S, Sharon LA, et al (2006) A nutrient uptake role for bacterial  
462 cell envelope extensions. *Proc Natl Acad Sci U S A* 103:11772–7.  
463 <https://doi.org/10.1073/pnas.0602047103>
- 464 13. Li G, Brown PJB, Tang JX, et al (2012) Surface contact stimulates the just-in-time  
465 deployment of bacterial adhesins. *Mol Microbiol* 83:41–51.  
466 <https://doi.org/10.1111/j.1365-2958.2011.07909.x>
- 467 14. Hug I, Deshpande S, Sprecher KS, et al (2017) Second messenger–mediated tactile  
468 response by a bacterial rotary motor. *Science* 358:531–534
- 469 15. Ellison CK, Dalia TN, Vidal Ceballos A, et al (2018) Retraction of DNA-bound type IV  
470 competence pili initiates DNA uptake during natural transformation in *Vibrio cholerae*.  
471 *Nat Microbiol* 3:773–780. <https://doi.org/10.1038/s41564-018-0174-y>
- 472 16. Ellison CK, Dalia TN, Dalia AB, Brun YV (2019) Real-time microscopy and physical  
473 perturbation of bacterial pili using maleimide-conjugated molecules. *Nat Protoc* 14:.  
474 <https://doi.org/10.1038/s41596-019-0162-6>
- 475 17. Shebelut CW, Guberman JM, van Teeffelen S, et al (2010) *Caulobacter* chromosome  
476 segregation is an ordered multistep process. *Proc Natl Acad Sci* 107:14194–14198.  
477 <https://doi.org/10.1073/pnas.1005274107>
- 478 18. Viollier PH, Sternheim N, Shapiro L (2002) Identification of a localization factor for the  
479 polar positioning of bacterial structural and regulatory proteins. *Proc Natl Acad Sci U S A*  
480 99:13831–6. <https://doi.org/10.1073/pnas.182411999>
- 481 19. Paul R, Jaeger T, Abel S, et al (2008) Allosteric Regulation of Histidine Kinases by Their  
482 Cognate Response Regulator Determines Cell Fate. *Cell* 133:452–461.  
483 <https://doi.org/10.1016/j.cell.2008.02.045>
- 484 20. Persat A, Nadell CD, Kim MK, et al (2015) The Mechanical World of Bacteria. *Cell*  
485 161:988–997. <https://doi.org/10.1016/J.CELL.2015.05.005>
- 486 21. Sanfilippo JE, Lorestani A, Koch MD, et al (2019) Microfluidic-based transcriptomics  
487 reveal force-independent bacterial rheosensing. *Nat Microbiol* 1.  
488 <https://doi.org/10.1038/s41564-019-0455-0>

- 489 22. Berne C, Ellison CK, Ducret A, Brun YV (2018) Bacterial adhesion at the single-cell  
490 level. *Nat Rev Microbiol* 16:616–627. <https://doi.org/10.1038/s41579-018-0057-5>
- 491 23. Kaczmarczyk A, Hempel AM, Arx C von, et al (2019) Precise transcription timing by a  
492 second-messenger drives a bacterial G1/S cell cycle transition. *bioRxiv* 675330.  
493 <https://doi.org/10.1101/675330>
- 494 24. Radhakrishnan SK, Thanbichler M, Viollier PH (2008) The dynamic interplay between a  
495 cell fate determinant and a lysozyme homolog drives the asymmetric division cycle of  
496 *Caulobacter crescentus*. *Genes Dev* 22:212–225. <https://doi.org/10.1101/gad.1601808>
- 497 25. Medico L Del, Cerletti D, Christen M, Christen B (2019) The type IV pilin PilA couples  
498 surface attachment and cell cycle initiation in *Caulobacter crescentus*. *bioRxiv* 766329.  
499 <https://doi.org/10.1101/766329>
- 500 26. Wagner JK, Brun YV (2007) Out on a limb: how the *Caulobacter* stalk can boost the study  
501 of bacterial cell shape. *Mol Microbiol* 64:28–33. [https://doi.org/10.1111/j.1365-](https://doi.org/10.1111/j.1365-2958.2007.05633.x)  
502 [2958.2007.05633.x](https://doi.org/10.1111/j.1365-2958.2007.05633.x)
- 503 27. Klein EA, Schlimpert S, Hughes V, et al (2013) Physiological role of stalk lengthening in  
504 *Caulobacter crescentus*. *Commun Integr Biol* 6:e24561. <https://doi.org/10.4161/cib.24561>
- 505 28. Poindexter JS (1964) Biological Properties and Classification of the *Caulobacter* Group.  
506 *Bacteriol Rev* 28:231–295
- 507 29. Ely B (1991) Genetics of *Caulobacter crescentus*. *Methods Enzymol* 204:372–384.  
508 [https://doi.org/10.1016/0076-6879\(91\)04019-K](https://doi.org/10.1016/0076-6879(91)04019-K)
- 509 30. Ried JL, Collmer A (1987) An *nptI-sacB-sacR* cartridge for constructing directed,  
510 unmarked mutations in gram-negative bacteria by marker exchange-*eviction* mutagenesis.  
511 *Gene* 57:239–46
- 512 31. Marks ME, Castro-Rojas CM, Teiling C, et al (2010) The genetic basis of laboratory  
513 adaptation in *Caulobacter crescentus*. *J Bacteriol* 192:3678–3688.  
514 <https://doi.org/10.1128/JB.00255-10>
- 515 32. Berne C, Ellison CK, Agarwal R, et al (2018) Feedback regulation of *Caulobacter*  
516 *crescentus* holdfast synthesis by flagellum assembly via the holdfast inhibitor HfiA. *Mol*  
517 *Microbiol* 110:219–238. <https://doi.org/10.1111/mmi.14099>
- 518 33. Severin GB, Waters CM (2017) Spectrophotometric and Mass Spectroscopic Methods for  
519 the Quantification and Kinetic Evaluation of In Vitro c-di-GMP Synthesis. In: *c-di-GMP*  
520 *Signaling*. Springer, pp 71–84
- 521 34. Massie JP, Reynolds EL, Koestler BJ, et al (2012) Quantification of high-specificity  
522 cyclic diguanylate signaling. *Proc Natl Acad Sci* 109:12746–12751
- 523 35. Ellison CK, Kan J, Chlebek JL, et al (2019) A bifunctional ATPase drives *tad* pilus  
524 extension and retraction. *bioRxiv* 616128. <https://doi.org/10.1101/616128>
- 525 36. Ellison CK, Rusch DB, Brun YV (2019) Flagellar mutants have reduced pilus synthesis in  
526 *Caulobacter crescentus*. *J Bacteriol* JB.00031-19. <https://doi.org/10.1128/jb.00031-19>

- 527 37. Evinger M, Agabian N (1977) Envelope-associated nucleoid from *Caulobacter crescentus*  
528 stalked and swarmer cells. *J Bacteriol* 132:294–301
- 529 38. Skerker JM, Shapiro L (2000) Identification and cell cycle control of a novel pilus system  
530 in *Caulobacter crescentus*. *EMBO J* 19:3223–3234.  
531 <https://doi.org/10.1093/emboj/19.13.3223>
- 532 39. Wheeler RT, Shapiro L (1999) Differential localization of two histidine kinases  
533 controlling bacterial cell differentiation. *Mol Cell* 4:683–94.  
534 [https://doi.org/10.1016/S1097-2765\(00\)80379-2](https://doi.org/10.1016/S1097-2765(00)80379-2)

535

536

537

538

539

540 **Supplemental Table 1. Strains, plasmids, and primers used in this study.**

541

Strain	Description or construction	Source or reference
<i>C. crescentus</i> Strains		
NA1000	<i>C. crescentus</i> lab-adapted strain	J. Poindexter, [37]
YB8288	NA1000 <i>pilA</i> <sup>T36C</sup>	[11]
YB0433	NA1000 <i>pilA</i> <sup>T36C</sup> <i>parB::mCherry-parB</i> (electroporated plasmid from strain YB7341 into YB8288)	This study
YB8773	NA1000 <i>pilA</i> <sup>T36C</sup> <i>pleC::pleC-yfp</i> (transduced lysate made from strain LS3205 into YB8288)	This study
YB8772	NA1000 <i>pilA</i> <sup>T36C</sup> <i>divJ::divJ-cfp</i> (transduced lysate made from strain LS3205 into YB8288)	This study
YB8455	NA1000 <i>pilA</i> <sup>T36C</sup> $\Delta$ <i>hfsDAB</i> (conjugated plasmid from strain YB3832 into YB8288)	This study
YB8459	NA1000 <i>pilA</i> <sup>T36C</sup> $\Delta$ <i>hfsDAB</i> <i>cpaC</i> <sup>G324D</sup> (conjugated plasmid from strain YB9097 into YB8455)	This study
YB8760	NA1000 <i>hfsA+</i> <i>pilA</i> <sup>T36C</sup> <i>parB::mCherry-parB</i> (electroporated plasmid from strain YB8776 into YB0433)	This study
YB8777	NA1000 <i>hfsA+</i> <i>pilA</i> <sup>T36C</sup> <i>cpaC</i> <sup>G324D</sup> <i>parB::mCherry-parB</i> (electroporated plasmid from strain YB8776 into YB8771)	This study

YB8771	NA1000 <i>pilA</i> <sup>T36C</sup> <i>cpaC</i> <sup>G324D</sup> <i>parB::mCherry-parB</i> (electroporated plasmid from strain YB7341 into YB8764)	This study
YB8764	NA1000 <i>pilA</i> <sup>T36C</sup> <i>cpaC</i> <sup>G324D</sup> (conjugated plasmid from strain YB9097 into YB8288)	This study
LS3118	NA1000 $\Delta$ <i>pilA</i>	[38]
YB8759	NA1000 <i>cpaC</i> <sup>G324D</sup> $\Delta$ <i>pilA</i> (conjugated plasmid from strain YB4030 into YB8764)	This study
LS3205	NA1000 <i>divJ::divJ-cfp</i> (Kan <sup>R</sup> ) / <i>pleC::pleC-yfp</i> (Spec/Strep <sup>R</sup> )	[39]

#### *E. coli* Strains

YB7341	$\alpha$ -select / pNPTS139 <i>parB::mCherry-parB</i>	D. Kysela
YB3832	S-17 / pNPTS138 $\Delta$ <i>hfsDAB</i>	
YB9097	S-17 / pNPTS138 <i>cpaC</i> <sup>G324D</sup>	This study
YB8776	$\alpha$ -select / pNPTS138 <i>hfsA</i> +	This study
YB4030	S-17 / pNPTS138 $\Delta$ <i>pilA</i>	[32]

#### Plasmids

pNPTS138	Litmus 38 derivative, <i>OriT SacB</i> ; Kan <sup>R</sup>	M.R.K Alley
pNPTS139	Litmus 39 derivative, <i>OriT SacB</i> ; Kan <sup>R</sup>	M.R.K. Alley
pNPTS139 <i>parB::mCherry-parB</i>	pNPTS139 containing ~500 bp fragment upstream of <i>parB</i> gene along with <i>mCherry</i> gene linked to <i>parB</i> at N-terminus	D. Kysela
pNPTS138 <i>cpaC</i> <sup>G324D</sup>	pNPTS138 containing 500 bp fragment upstream and downstream of <i>cpaC</i> <sup>G324D</sup> mutation	This study
pNPTS138 <i>hfsA</i> +	pNPTS138 containing entire <i>hfsA</i> gene flanked by 500 bp upstream and 580 bp downstream of coding region	This study

#### Primers

#### Sequence

#### Description

	lower case – overlapping sequence with plasmid UPPER CASE – <i>C. crescentus</i> DNA segment <b><u>Bold/Underline – Mutation built into primer</u></b>	
cpaCG324DUpF	ttctggatccacgatCGGTGGACCAACTGGCCGCGATGCT	Construction of pNPTS138 <i>cpaC</i> <sup>G324D</sup>
cpaCG324UpR	TTCAGGCCCGGGTCTGTCGGCGGTGCTCTGGA	Construction of pNPTS138 <i>cpaC</i> <sup>G324D</sup>
cpaCG324DownF	CCAGAGCACCGCCGACGACCCGGGCTGAAC	Construction of pNPTS138 <i>cpaC</i> <sup>G324D</sup>
cpaCG324DownR	agcttcctgcaggatAGGAAGTCGCGGAGCGGAACAGCG	Construction of pNPTS138 <i>cpaC</i> <sup>G324D</sup>
pNPTShfsAF	ttctggatccacgatCCTCGCCGCCACGAACACCTTC	Construction of pNPTS138 <i>hfsA</i> +
pNPTShfsAR	agcttcctgcaggatGCCCGCCAGTAGTCCGGCGACG	Construction of pNPTS138 <i>hfsA</i> +

542

543

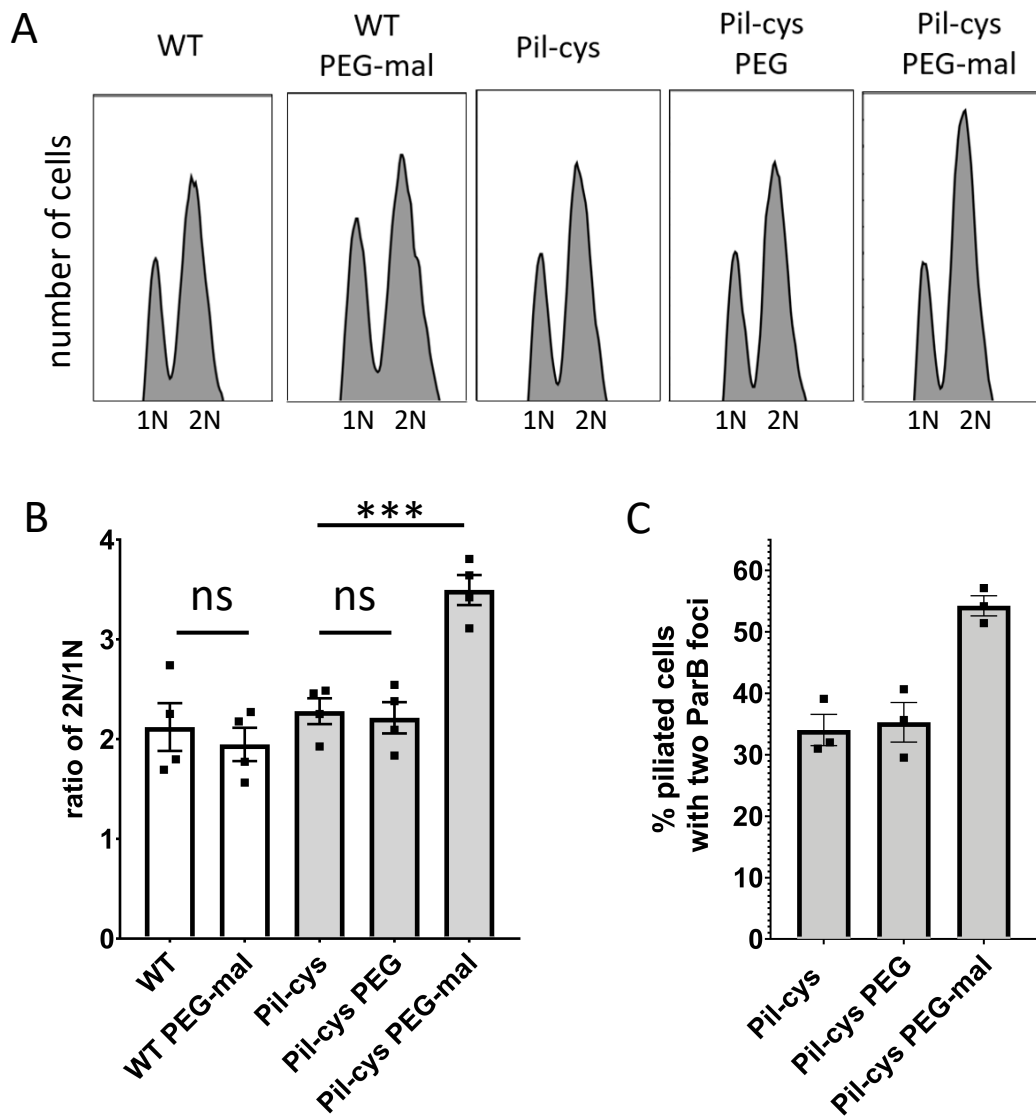


**Figure 1.** Obstruction of pilus retraction stimulates DNA replication initiation. (A) Representative flow cytometry plots showing chromosome content of cells quantified in (B). (B) Ratio of cells with two chromosomes (2N) to cells with one chromosome (1N) determined by flow cytometry analysis of genomic content. Bar graph shows the mean  $\pm$  SEM of three independent, biological replicates. (C) Quantification of the percent of pilated cells with two ParB-mCherry foci. Bar graph shows the mean  $\pm$  SEM of three independent, biological replicates. A minimum of 100 cells was quantified for each replicate. Statistical comparisons were made using Sidak's multiple comparisons test. WT = wild type. \*\*\* $P < 0.001$ , ns = not significant.



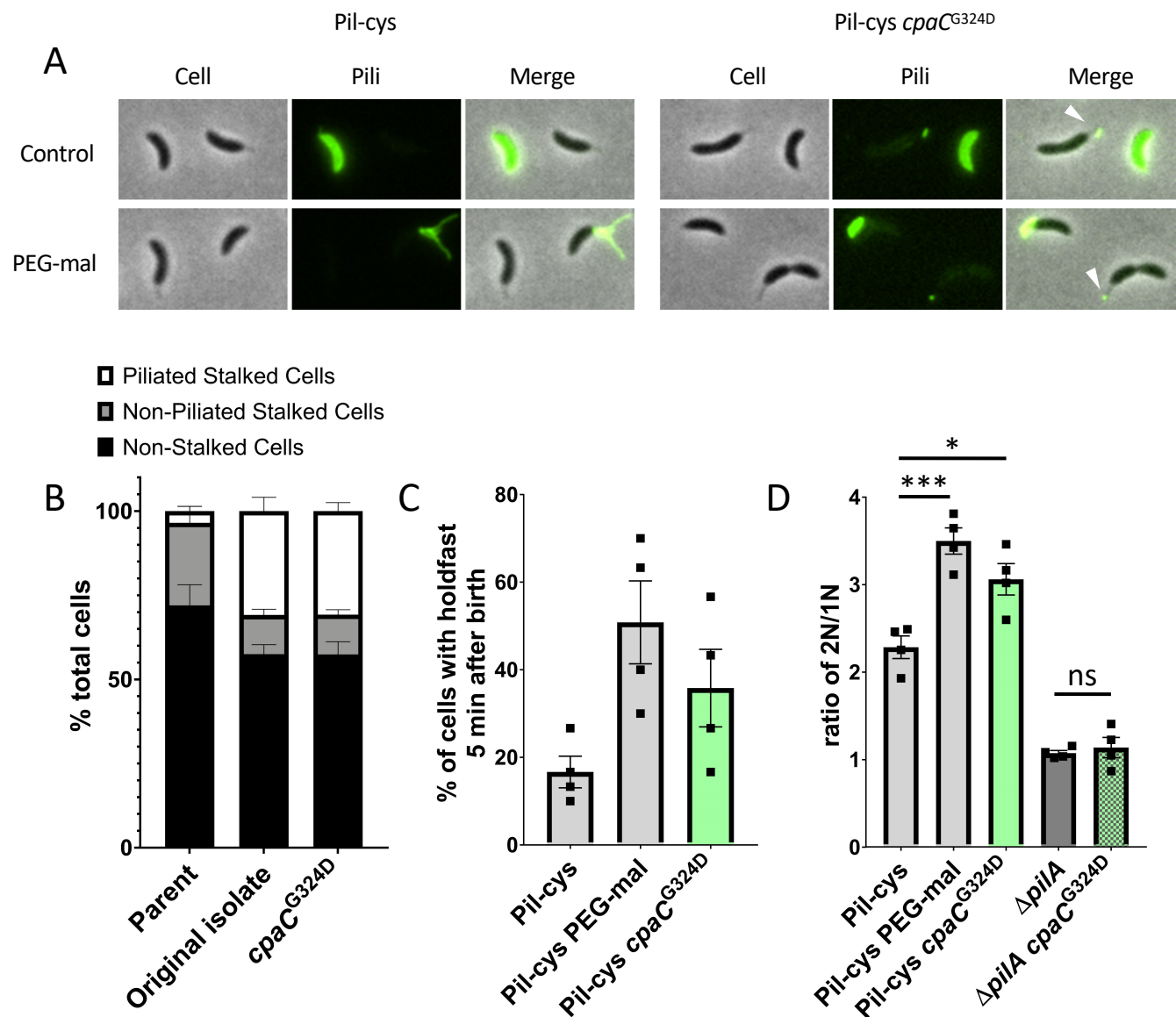


**Figure 2.** A mutation in the CpaC outer membrane pilus secretin partially obstructs pilus retraction and stimulates cell cycle progression and cellular differentiation. (A) Representative images of Pil-cys parent and strain containing *cpaC*<sup>G324D</sup> mutation. Arrows indicate stalks with labeled pilus fibers attached to them. (B) Quantification of piliated stalk phenotype shown in (A). Data are from four independent, biological replicates and bar graphs show mean  $\pm$  SEM. (C) Percent of synchronized cells that have made a holdfast by the start of the imaging experiment five min after birth. Bar graphs show mean  $\pm$  SEM. Data are from four independent, biological replicates ( $n = 30$  cells per replicate). (D) Ratio of cells with two chromosomes (2N) to cells with one chromosome (1N) determined by flow cytometry analysis of genomic content. Bar graph shows the mean  $\pm$  SEM of four independent, biological replicates. Statistical comparisons were made using Sidak's multiple comparisons test. \* $P < 0.05$ , \*\*\* $P < 0.001$ , \*\*\*\* $P < 0.0001$ .

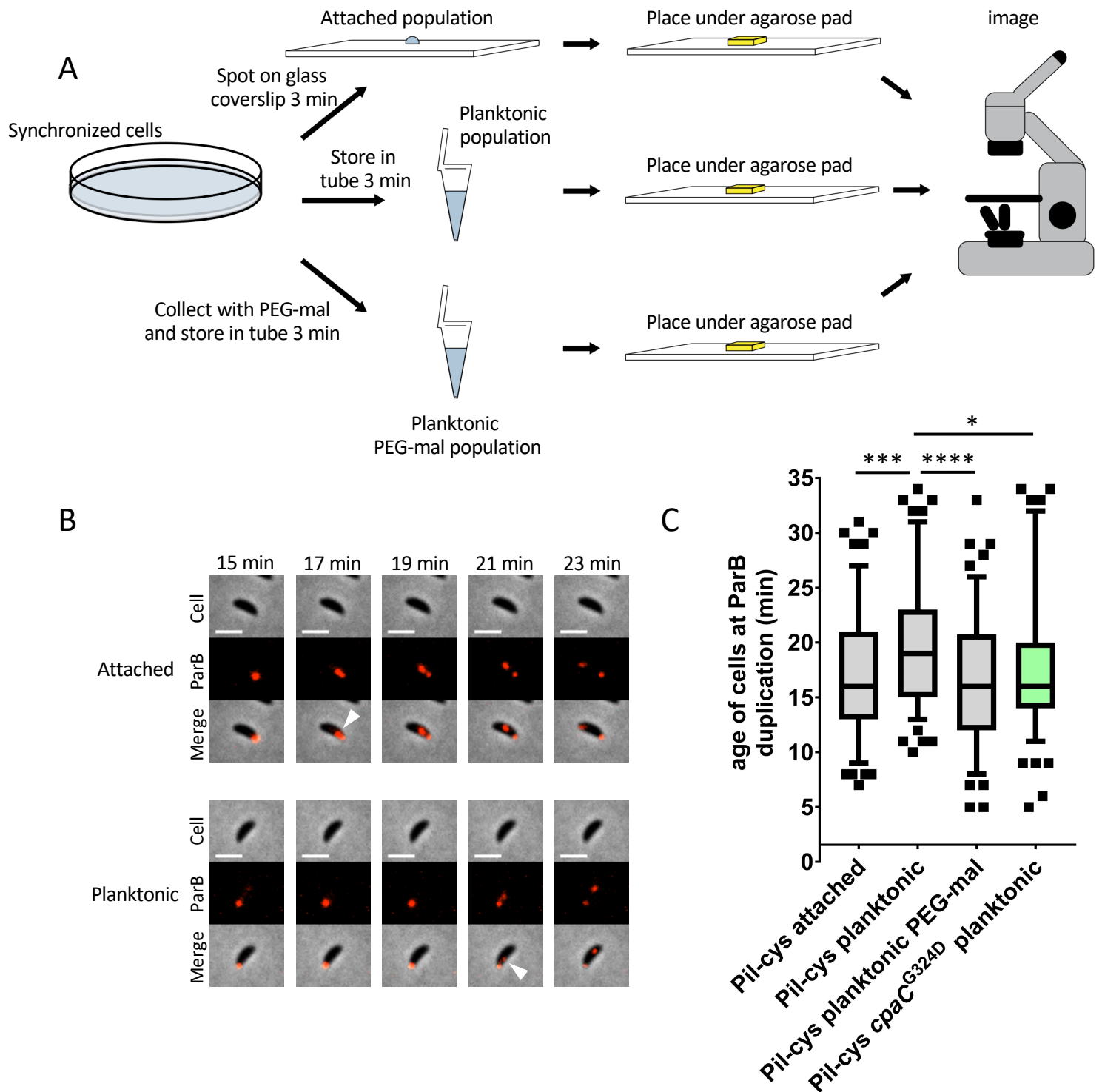


**Figure 3.** Surface contact stimulates cell cycle progression. (A) Schematic of experimental setup. (B) Representative time-lapse images of data shown in (C). Scale bars are 2  $\mu$ m. White arrows indicate ParB duplication event. (C) Box and whisker plots show 5-95% confidence interval. Data are compiled from four independent, biological replicates ( $n = 30$  cells per replicate). Statistical comparisons were made using Sidak's multiple comparisons test. \* $P < 0.05$ , \*\*\* $P < 0.001$ , \*\*\*\* $P < 0.0001$ .

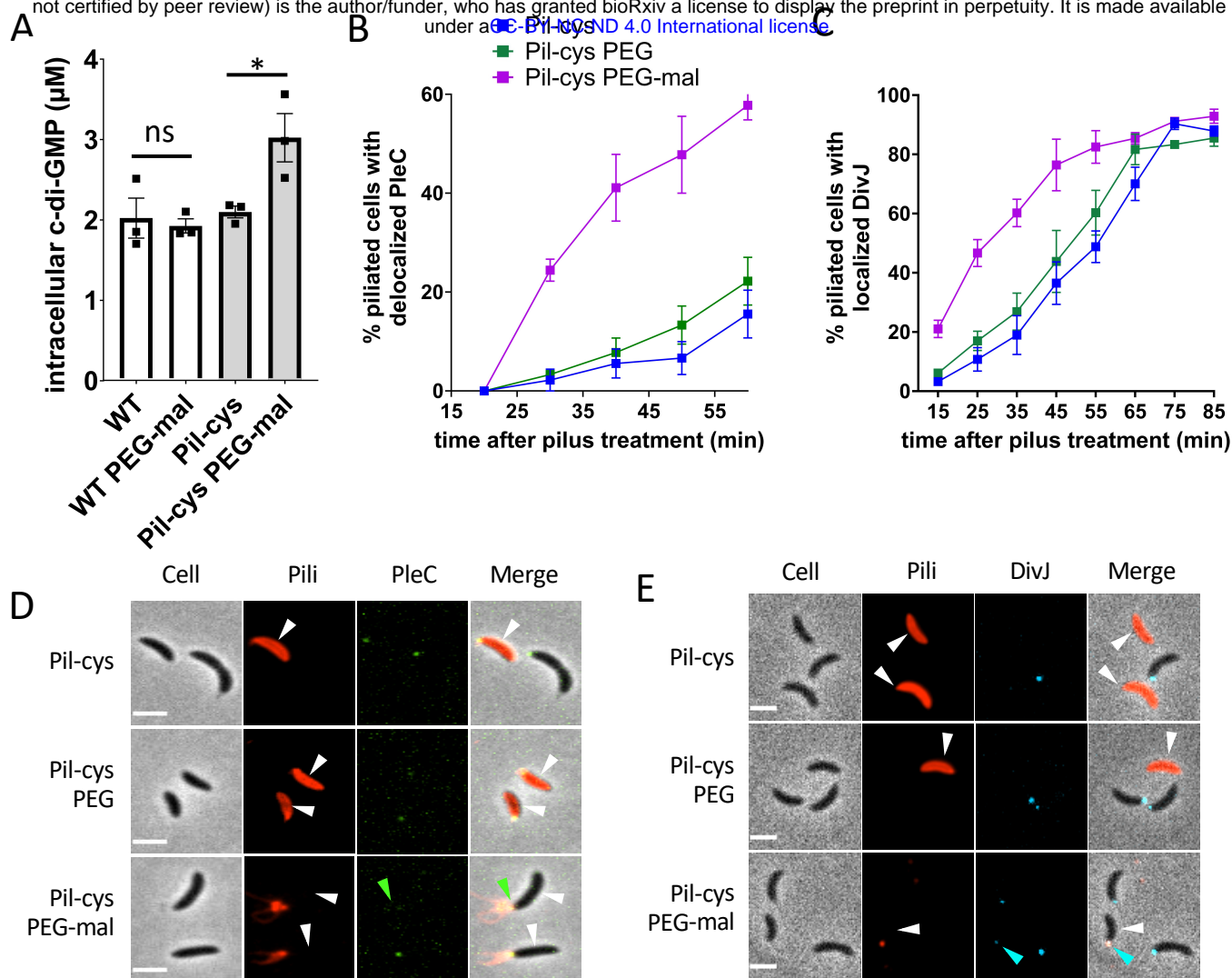


**Figure 4.** Obstruction of pilus retraction stimulates c-di-GMP synthesis by altering activity of developmental regulators. (A) Quantification of intracellular c-di-GMP concentrations of wild type and Pil-cys strains with PEG-mal treatment. Bar graph shows the mean  $\pm$  SEM of three independent, biological replicates. Statistical comparisons were made using Sidak's multiple comparisons test. WT = wild type. \* $P < 0.05$ , ns = not significant. (B) Percent of piliated cells with localized PleC at each time point. Error bars indicate mean  $\pm$  SEM of three independent, biological replicates ( $n =$  at least 30 cells per replicate per time point). (C) Percent of piliated cells with localized DivJ at each time point. Error bars indicate mean  $\pm$  SEM of four independent, biological replicates ( $n =$  at least 30 cells per replicate per time point). (D) Representative microscopy images of cells from data shown in (B). Green arrow represents delocalized PleC at the piliated pole. (E) Representative microscopy images of cells at the 25 min time point of data shown in (C). Blocked pili in Pil-cys PEG-mal treated samples appear as puncta due to shearing of filaments. Blue arrow indicates DivJ localization in piliated cell. White arrows indicate piliated cells. Scale bars are 2  $\mu$ m.

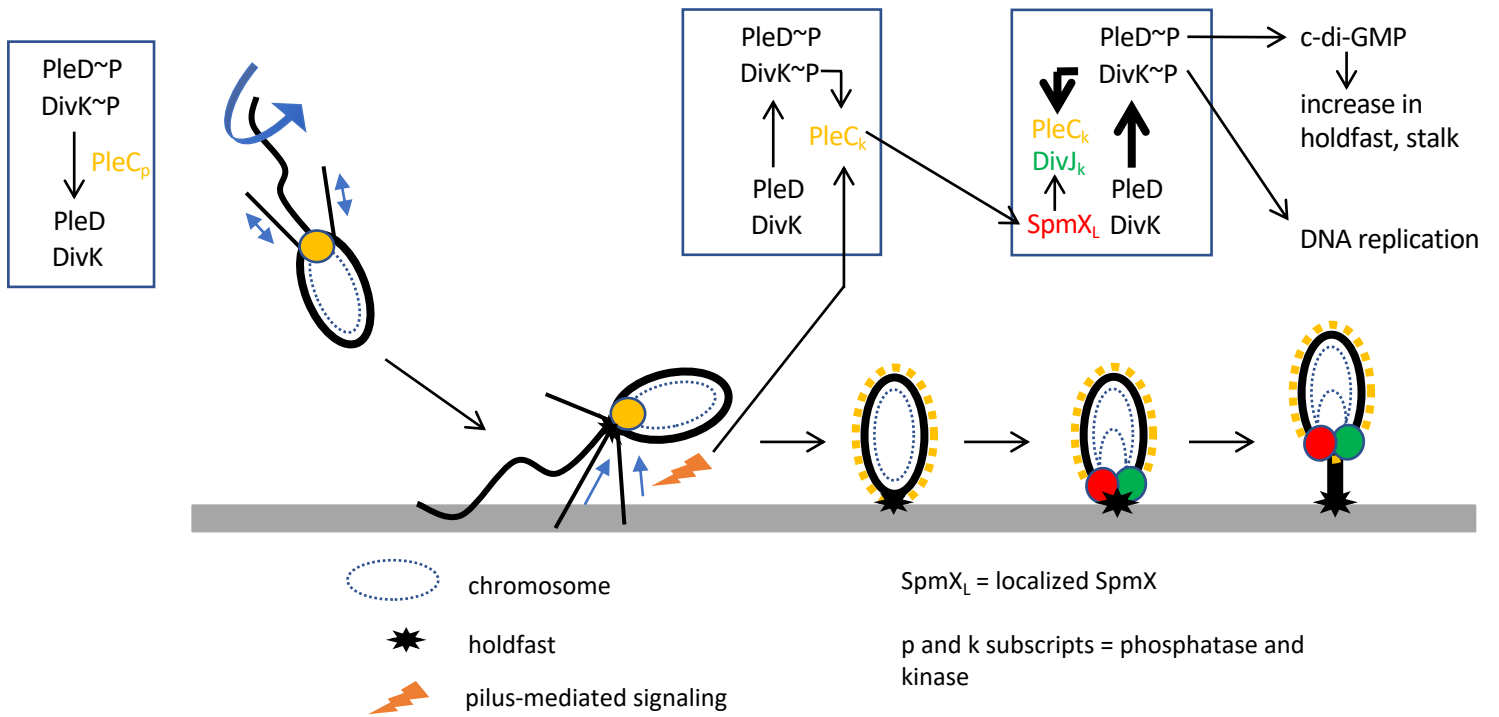


**Figure 5.** Model of cell cycle acceleration upon surface contact. Surface sensing through alterations in pilus retraction upon surface binding stimulates the PleC switch from phosphatase to kinase activities of PleC which occurs upon PleC delocalization. This in turn stimulates the localization of SpmX which recruits the kinase DivJ. DivJ phosphorylates PleD and DivK, resulting in the production of c-di-GMP and the stimulation of DNA replication respectively. Increased c-di-GMP production from phosphorylated PleD results in more holdfast synthesis and stalk growth.